RSC Advances

RSC Publishing

COMMUNICATION

Enhanced visible-light photocatalytic degradation of methyl orange by $BiPO_4$–CdS composites synthesized using a microwave-assisted method

Cite this: *RSC Advances*, 2012, 2, 12706–12709

Received 6th July 2012,
Accepted 24th October 2012

DOI: 10.1039/c2ra21382f

www.rsc.org/advances

Tian Lv, Likun Pan,* Xinjuan Liu and Zhuo Sun

$BiPO_4$–CdS composites consisting of $BiPO_4$ nanorods and CdS nanoparticles were successfully synthesized *via* a microwave-assisted reaction. The photocatalytic performance of the $BiPO_4$–CdS composites, with different proportions of CdS, in the degradation of methyl orange under visible light irradiation was investigated. The results show that the $BiPO_4$–CdS composite with 30.1 wt% CdS achieves a better performance with a maximum degradation rate of 98.1% as compared with pure $BiPO_4$ due to the increase of specific surface area for more adsorbed MO, the enhancement of light absorption and the reduction of carrier recombination.

Semiconductor oxide photocatalysis has attracted much attention for water treatment due to its good destruction ability of pollutants and broad compound applicability.[1–4] Among various semiconductor oxide photocatalysts, TiO_2 has been used widely for environmental applications due to its intriguing optical and electric properties, low cost, nontoxicity, and ease of availability.[5–7] However, the photocatalytic activity of TiO_2 is not high enough to meet the need of industrial usages due to the rapid recombination of photogenerated electrons and holes, which causes high running costs.[8]

Recently, $BiPO_4$ has been recognized as an excellent photocatalyst with superior photocatalytic activity to P25 (the commercial TiO_2) in the UV region when used for the destruction of dyes and pollutants.[8–12] Liu *et al.* obtained $BiPO_4$ nanorods *via* a hydrothermal method and the $BiPO_4$ nanorods showed a high efficiency in the photocatalytic degradation of methylene blue (MB) under UV light irradiation.[9] Pan and Zhu synthesized $BiPO_4$ nanocrystals by a high-temperature hydrolysis reaction and the $BiPO_4$ nanocrystals exhibited high activity in the degradation of MB under UV light irradiation.[12] However, similar to TiO_2, the wide band gap of $BiPO_4$ (~3.85 eV) limits its photocatalytic property to the UV region, which only occupies 3–5% of the total solar spectrum.[13,14] To improve the sunlight photocatalytic efficiency, many promising studies have reported the coupling of TiO_2 with a narrow band gap semiconductor material, typically CdS (2.4 eV), to extend the absorption to the visible light range.[15–19] In the meantime, the photoexcited electrons in CdS can be efficiently injected into TiO_2 because the conduction band (CB) level of CdS is higher than that of TiO_2.[20,21] Similarly, the combination of $BiPO_4$ and CdS should be an ideal system to achieve good photocatalytic performance under visible light irradiation. Firstly, CdS can extend the optical response to the visible light range. Secondly, as shown in Fig. 1, on the basis of the relevant band positions of $BiPO_4$ and CdS (CB: −4.07 eV and −3.98 eV *vs.* vacuum),[8,22] photo-induced electrons easily transfer from CdS CB to $BiPO_4$ CB, which could efficiently separate the photo-induced electrons and hinder the charge recombination in electron-transfer processes. Unfortunately, there has been no report on the synthesis and investigation of $BiPO_4$–CdS composites for photocatalysis until now.

In this work, a simple synthesis of $BiPO_4$–CdS composites was carried out through a microwave-assisted reaction for the first

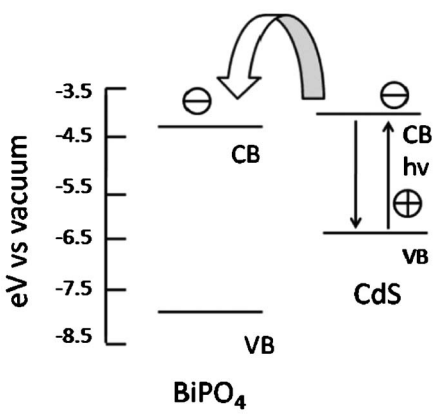

Fig. 1 Schematic diagram of energy levels of $BiPO_4$ and CdS. CB and VB are the conduction band and valence band, respectively.

Engineering Research Center for Nanophotonics & Advanced Instrument, Ministry of Education, Department of Physics, East China Normal University, Shanghai 200062, China. E-mail: lkpan@phy.ecnu.edu.cn; Fax: +86 21 62234321; Tel: +86 21 62234132

time. Microwave irradiation heats the reactant to a high temperature in a short time by transferring energy selectively to microwave absorbing polar solvents.[23,24] Thus it can facilitate mass production in a short time span with little energy consumption[25,26] and form an intimate contact between the components,[27,28] which is crucial for the formation of electronic interaction and interelectron transfer at the interface. The as-synthesized $BiPO_4$–CdS composites exhibit an enhanced photocatalytic performance in the degradation of methyl orange (MO) under visible light irradiation as compared with pure $BiPO_4$.

1 mmol $Bi(NO_3)_3{\cdot}5H_2O$ and 1 mmol $Na_3PO_4{\cdot}12H_2O$ were added in 20 mL distilled water and magnetically stirred to form a homogeneous solution at room temperature. The solution was then put into an automated focused microwave system (Explorer-48, CEM Co.) and treated at 150 °C with a microwave irradiation power of 100 W for 15 min. The as-synthesized $BiPO_4$ was isolated by filtration, washed several times with distilled water, and finally dried in a vacuum oven at 60 °C for 24 h.

Different amounts of $CdCl_2{\cdot}2.5H_2O$ and $Na_2S{\cdot}9H_2O$ (Sinopharm Chemical Reagents Co. Ltd.) were added into the as-prepared $BiPO_4$ suspensions and then the solutions were sonicated for 30 min to produce uniform dispersions and were then treated at 100 °C with a microwave irradiation power of 100 W for 5 min. The as-synthesized $BiPO_4$–CdS samples with 8.9, 16.4, 30.1 and 45.5 wt% CdS, named as BC-1, BC-2, BC-3 and BC-4, were isolated by filtration, washed several times with distilled water, and finally dried in a vacuum oven at 60 °C for 24 h.

The surface morphology, structure and composition of the samples were characterized by field-emission scanning electron microscopy (FESEM, Hitachi S-4800), high-resolution transmission electron microscope (HRTEM, JEOL-2010), energy dispersive X-ray spectroscopy (EDS, JEM-2100) and X-ray diffraction spectroscopy (XRD, Holland Panalytical PRO PW3040/60) with Cu-Kα radiation (V = 30 kV, I = 25 mA), respectively. The Brunauer–Emmett–Teller (BET) specific surface areas of the samples were evaluated on the basis of nitrogen adsorption isotherms measured at 77 K using a ASAP 2010 apparatus (Micromeritics, U.S.A). All the samples were degassed at 160 °C before nitrogen adsorption measurements. The BET surface area was determined using the adsorption data in the relative pressure (P/P_0) range of 0.025–0.999. The UV-vis absorption spectra were recorded using a Hitachi U-3900 UV-vis spectrophotometer.

The photocatalytic performance of the as-prepared samples was evaluated by photocatalytic degradation of MO under visible light irradiation. 150 mg $BiPO_4$–CdS powders were added into 100 mL MO aqueous solutions (10 mg L^{-1}). The mixed suspension was continuously stirred for 0.5 h in the dark to reach an adsorption–desorption equilibrium. Under ambient conditions and stirring, the mixed suspension was exposed to the visible irradiation produced by a 400 W metal halogen lamp with cut off filter ($\lambda > 400$ nm). At certain time intervals, 2 mL of the mixed suspension was extracted and centrifugated to remove the photocatalyst. The degradation process was monitored by measuring the absorption of MO in the filtrate at 463 nm using an UV-vis absorption spectrometer.

The FESEM images of $BiPO_4$, BC-1, BC-2, BC-3 and BC-4 are shown in Fig. 2(a)–(e). The $BiPO_4$ nanorod is 600–700 nm in length and 100–200 nm in width. It can be observed from Fig. 2(b) that a small amount of CdS has been distributed on the surface of $BiPO_4$ as compared with bare $BiPO_4$ nanorods [Fig. 2(a)]. A more compact surface is observed from Fig. 2(c)–(e), indicating that more CdS nanoparticles have been deposited on the surface of $BiPO_4$. The existence of CdS and $BiPO_4$ in the composite has been proved by the peaks of Cd, S, Bi, P and O in EDS data [Fig. 2(f)]. The BET specific surface areas of $BiPO_4$, BC-1, BC-2, BC-3 and BC-4 are found to be 4.1, 35.9, 50.0, 56.3 and 47.0 $m^2\ g^{-1}$, respectively, indicating that the increase of CdS can supply more surface sites to accommodate more adsorbed MO, which is beneficial to the photocatalytic degradation of MO. However, excessive loading of CdS nanoparticles may cause their aggregation, as indicated from the morphology of the BC-4 sample in Fig. 2(e), and thus decreases the specific surface area.

The low-magnification and high-magnification HRTEM images of BC-3 are shown in Fig. 3(a) and (b). It is clearly found from Fig. 3(a) that the surface of the $BiPO_4$ nanorods is decorated with CdS nanoparticles. The large crystallites are identified to be $BiPO_4$ nanorods, as shown in Fig. 3(b). The lattice spacing measured for the crystalline plane is 0.442 nm, corresponding to the (101) plane of the hexagonal phase $BiPO_4$ (JCPDS#45-1370).[11] Around the $BiPO_4$ crystallite edge, fine crystallites are observed. The crystallites connecting to the $BiPO_4$ have lattice fringes of 0.335 nm, which is ascribed to the (111) plane of CdS (JCPDS#80-0019). The HRTEM

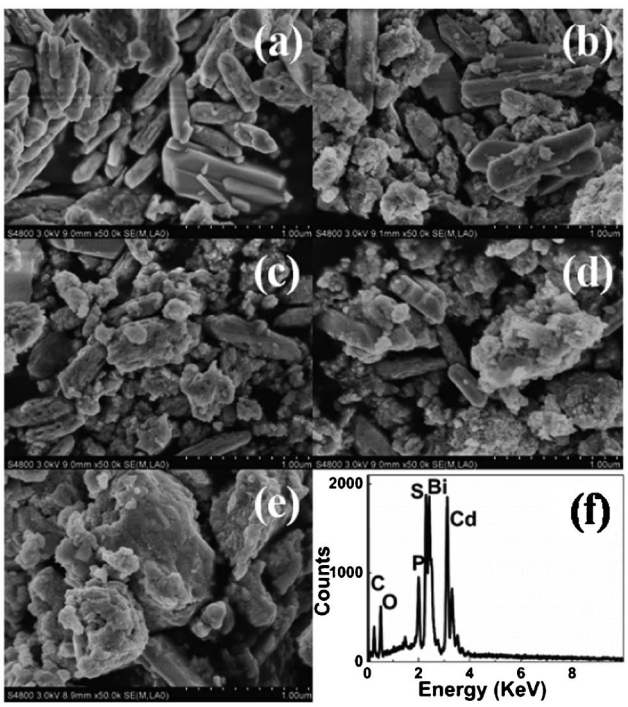

Fig. 2 FESEM images of (a) $BiPO_4$ (b) BC-1, (c) BC-2, (d) BC-3 and (e) BC-4; (f) EDS spectrum of BC-3.

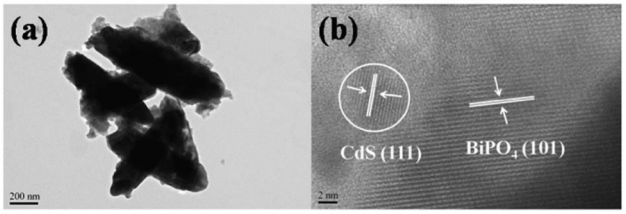

Fig. 3 (a) Low-magnification and (b) high-magnification HRTEM images of BC-3.

image also indicates that CdS, with a size of about 5 nm is presented in a crystalline structure.

The XRD patterns of $BiPO_4$, BC-1, BC-2, BC-3 and BC-4 are shown in Fig. 4. Compared with the XRD pattern of $BiPO_4$, in which several peaks correspond to hexagonal and monoclinic phases of $BiPO_4$ (JCPDS#45-1370, JCPDS#80-0209), three main peaks corresponding to the (111), (220) and (311) planes of CdS (JCPDS#80-0019) appear in other XRD patterns. This further confirms the existence of CdS on $BiPO_4$. The signals corresponding to CdS indicate the CdS crystallites are mainly present as a cubic structure and their relative intensity increases with the increase of CdS amount.

Fig. 5(a) shows the UV-vis absorption spectra of $BiPO_4$, BC-1, BC-2, BC-3 and BC-4. Compared with the spectrum of $BiPO_4$, there is an obvious absorption peak near 500 nm for $BiPO_4$–CdS composites, which is ascribed to the contribution from CdS. The band gap of the CdS QDs, corresponding to the absorption edge, is about 2.38 eV. The gradual increase of absorbance from BC-1 to BC-4 shows that more CdS has been attached onto the surface of $BiPO_4$, which is similar to those reported in TiO_2–CdS composites.[29] This result is consistent with the FESEM observation. The photocatalytic degradation of MO under visible light irradiation was used to evaluate the photocatalytic performance of $BiPO_4$, BC-1, BC-2, BC-3 and BC-4, as shown in Fig. 5(b). It was observed that MO is hardly degraded under visible light in the absence of the

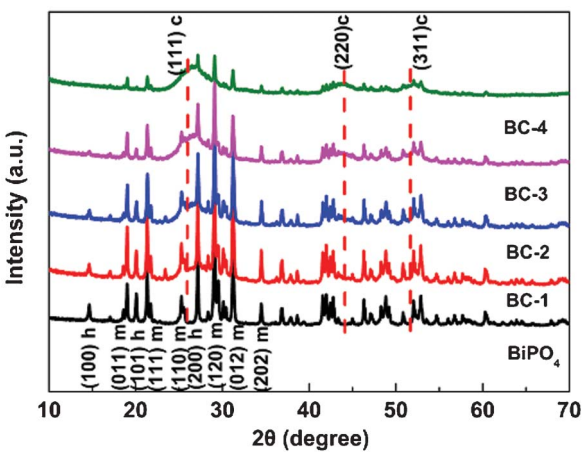

Fig. 4 XRD patterns of $BiPO_4$, BC-1, BC-2, BC-3 and BC-4. c –cubic CdS, h – hexagonal and m – monoclinic $BiPO_4$.

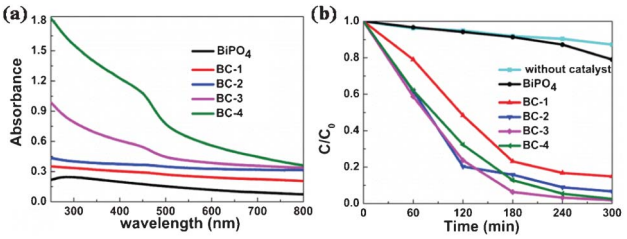

Fig. 5 (a) UV-vis absorption spectra of $BiPO_4$, BC-1, BC-2, BC-3 and BC-4; (b) photocatalytic degradation of MO by $BiPO_4$, BC-1, BC-2, BC-3 and BC-4 under visible light irradiation.

photocatalyst. Only 21.1% MO can be photodegraded by pure $BiPO_4$ under visible light in 5 h. However, all $BiPO_4$–CdS composites exhibit a better photocatalytic performance than pure $BiPO_4$. When CdS is introduced into $BiPO_4$, the degradation rate is increased to 85.1% and 93.4% for BC-1 and BC-2 and reaches a maximum value of 98.1% for BC-3, which is due to the increased specific surface area that supplies more surface sites to accommodate more adsorbed MO, the enhanced light absorption and the stepwise structure of the energy levels constructed in the $BiPO_4$–CdS composite (Fig. 1). However, when the loading amount of CdS is further increased, the photocatalytic performance deteriorates. This is ascribed to the following reasons: (i) it will be more difficult to transport an electron from CdS into $BiPO_4$ at a high CdS loading because of the increase in the average distance and electron injection time from CdS to $BiPO_4$;[30] (ii) more CdS content would reduce the specific surface area of $BiPO_4$ to adsorb MO;[31] (iii) charge carriers dissipate by trapping when the loading amount of CdS comes up to a certain level.[32]

The specific surface area of the photocatalyst plays an important role in photocatalytic degradation.[33] The larger the surface area of the photocatalyst, the more reaction sites there are, which is in favor of the photocatalytic activity.[34] In order to rule out the effect of specific surface areas on the photocatalytic activities, the photocatalytic reaction rates should be normalized by the specific surface areas.[35–37] Zhang *et al.*[38] investigated the reaction rate constants (k) and k' (k values normalized by the surface areas) of BiOI in the MO degradation and found that the order for the k' was the same as that of the original k. Fig. 6 shows the linear fitting using the pseudo-first-order kinetic equations to the experimental data for $BiPO_4$, BC-1, BC-2, BC-3 and BC-4. The values of k can be obtained directly from the fitted straight-line plots of $\ln(C_i/C_0)$ *versus* reaction time, which follow the order: BC-3 (0.0134 min^{-1}) > BC-4 (0.0105 min^{-1}) > BC-2 (0.0098 min^{-1}) > BC-1 (0.0068 min^{-1}) > $BiPO_4$ (0.00067 min^{-1}). The k' (normalized k) values are 0.00016 g min^{-1} m^{-2}, 0.00019 g min^{-1} m^{-2}, 0.0002 g min^{-1} m^{-2}, 0.00024 g min^{-1} m^{-2}, and 0.00022 g min^{-1} m^{-2} for $BiPO_4$, BC-1, BC-2, BC-3 and BC-4, respectively. The results indicate that the order of the normalized rates is the same as that of the original rates, which is similar to that reported in the literature.[38] The enhanced photocatalytic activity with the increase of CdS content should be ascribed to the enhanced light absorption. BC-3 exhibits the best photocatalytic activity. The

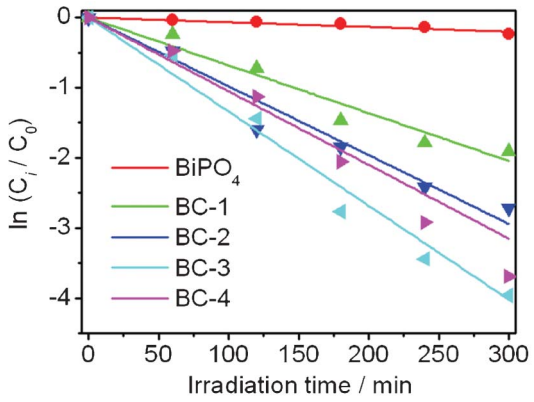

Fig. 6 Photocatalytic reaction kinetics of MO with reaction time.

photocatalytic activity of BC-4 is worse than that of BC-3 due to the more difficult electron transport and the charge carriers dissipate by trapping when the loading amount of CdS comes up to a certain level.[30,32]

In summary, we have demonstrated a simple, rapid and effective microwave-assisted method to synthesize $BiPO_4$–CdS composites for the degradation of MO. The results of the photocatalytic experiments indicate that (i) the $BiPO_4$–CdS composites exhibit better photocatalytic performances than pure $BiPO_4$ under visible light irradiation; (ii) the photocatalytic performances of the $BiPO_4$–CdS composites is dependent on the proportion of CdS, and the composite with 30.1 wt% CdS achieves the highest degradation rate of 98.1% for the degradation of MO; (iii) the enhanced photocatalytic performance is ascribed to the increase of the specific surface area for more adsorbed MO, the enhancement of light absorption and the reduction of carrier recombination.

References

1 G. L. Xiang, D. Wu, J. He and X. Wang, *Chem. Commun.*, 2011, **47**, 11456.
2 Z. G. Xiong, L. L. Zhang, J. Z. Ma and X. S. Zhao, *Chem. Commun.*, 2010, **46**, 6099.
3 P. Ma, Y. Wu, Z. Fu and W. Wang, *J. Alloys Compd.*, 2011, **509**, 3576.
4 D. Zhang, X. Liu and X. Wang, *J. Alloys Compd.*, 2011, **509**, 4972.
5 M. Y. Guo, M. K. Fung, F. Fang, X. Y. Chen, A. M. C. Ng, A. B. Djurisic and W. K. Chan, *J. Alloys Compd.*, 2011, **509**, 1328.
6 X. Zeng, Y. X. Gan, E. Clark and L. Su, *J. Alloys Compd.*, 2011, **509**, L221.
7 J. Zhang, Y. P. Zhang, Y. K. Lei and C. X. Pan, *Catal. Sci. Technol.*, 2011, **1**, 273.
8 C. S. Pan and Y. F. Zhu, *Environ. Sci. Technol.*, 2010, **44**, 5570.
9 Y. F. Liu, X. G. Ma, X. Yi and Y. F. Zhu, *Acta Phys. Chim. Sin.*, 2012, **28**, 654.
10 C. S. Pan, J. Xu, Y. Chen and Y. F. Zhu, *Appl. Catal., B*, 2012, **115–116**, 314.
11 G. F. Li, Y. Ding, Y. F. Zhang, Z. Lu, H. Z. Sun and R. Chen, *J. Colloid Interface Sci.*, 2011, **363**, 497.
12 C. S. Pan and Y. F. Zhu, *J. Mater. Chem.*, 2011, **21**, 4235.
13 S. U. Khan, M. Al-Shahry and W. B. Jr, *Science*, 2002, **297**, 2243.
14 Z. G. Zou, J. H. Ye, K. Sayama and H. Arakawa, *Nature*, 2001, **414**, 625.
15 Q. Li, T. Kako and J. Ye, *J. Mater. Chem.*, 2010, **20**, 10187.
16 Y. Xie, G. Ali, S. H. Yoo and S. O. Cho, *ACS Appl. Mater. Interfaces*, 2010, **2**, 2910.
17 S. C. Hayden, N. K. Allam and M. A. El-Sayed, *J. Am. Chem. Soc.*, 2010, **132**, 14406.
18 J. Bai, J. Li, Y. Liu, B. Zhou and W. Cai, *Appl. Catal., B*, 2010, **95**, 408.
19 A. H. Zyoud, N. Zaatar, I. Saadeddin, C. Ali, D. Park, G. Campet and H. S. Hilal, *J. Hazard. Mater.*, 2010, **173**, 318.
20 T. Lv, L. K. Pan, X. J. Liu, T. Lu, G. Zhu, Z. Sun and C. Q. Sun, *Catal. Sci. Technol.*, 2012, **2**, 754.
21 G. Zhu, F. F. Su, T. Lv, L. K. Pan and Z. Sun, *Nanoscale Res. Lett.*, 2010, **5**, 1749.
22 M. Grätzel, *Nature*, 2001, **414**, 338.
23 T. Lv, L. K. Pan, X. J. Liu, T. Lu, G. Zhu and Z. Sun, *J. Alloys Compd.*, 2011, **509**, 10086.
24 Y. C. Chen, S. L. Lo, H. H. Ou and C. H. Chen, *Water Sci. Technol.*, 2011, **63**, 550.
25 G. Zhu, L. K. Pan, T. Xu, Q. Zhao, B. Lu and Z. Sun, *Nanoscale*, 2011, **3**, 2188.
26 S. Horikoshi, H. Abe, K. Torigoe, M. Abe and N. Serpone, *Nanoscale*, 2010, **2**, 1441.
27 X. J. Liu, L. K. Pan, T. Lv, G. Zhu, Z. Sun and C. Q. Sun, *Chem. Commun.*, 2011, **47**, 11984.
28 G. Zhu, L. K. Pan, T. Xu, Q. Zhao and Z. Sun, *ACS Appl. Mater. Interfaces*, 2011, **3**, 1472.
29 L. Wu, J. C. Yu and X. Z. Fu, *J. Mol. Catal. A: Chem.*, 2006, **244**, 25.
30 N. Guijarro, T. Lana-Villarreal, Q. Shen, T. Toyoda and R. Gomez, *J. Phys. Chem. C*, 2010, **114**, 21928.
31 L. Ge and J. Liu, *Appl. Catal., B*, 2011, **105**, 289.
32 A. E. Raevskaya, A. L. Stroyuk, G. Ya. Grodzyuk, S. Ya. Kuchmii, V. M. Dzhagan, V. F. Plyusnin and V. P. Grivin, *Theor. Exp. Chem.*, 2010, **46**, 273.
33 M. Hermanek, R. Zboril, I. Medrik, J. Pechousek and C. Gregor, *J. Am. Chem. Soc.*, 2007, **129**, 10929.
34 V. Stengl and S. Bakardjieva, *J. Phys. Chem. C*, 2010, **114**, 19308.
35 G. Liu, Y. N. Zhao, C. H. Sun, F. Li, G. Q. Lu and H. M. Cheng, *Angew. Chem., Int. Ed.*, 2008, **47**, 4516.
36 W. Li, Y. Bai, W. J. Liu, C. Liu, Z. H. Yang, X. Feng, X. H. Lu and K.Y. Chan, *J. Mater. Chem.*, 2011, **21**, 6718.
37 Q. Sun and Y. M. Xu, *J. Phys. Chem. C*, 2010, **114**, 18911.
38 X. Zhang and L. Z. Zhang, *J. Phys. Chem. C*, 2010, **114**, 18198.